Dynamic Cross-Layer Transmission Control for Station-Assisted Satellite Networks

Changhee Joo* and Jihwan P. Choi†
*School of Electrical and Computer Engineering,
Ulsan National Institute of Science and Technology (UNIST), Korea
†Dept. of Information and Communication Eng.
Daegu Gyeongbuk Institute of Science & Technology (DGIST), Korea
Email: cjoo@unist.ac.kr, jhchoi@dgist.ac.kr

***Abstract*—In addition to sending signals directly to end user terminals, the multibeam satellite can benefit from path-diversity by routing to ground stations, which will relay signals to the end users through terrestrial networks. We investigate a cross-layer dynamic transmission control in station-assisted satellite networks, and develop an optimal solution that is amenable to implement with simple queue structure. We demonstrate the impact of ground stations and power control on the performance of multibeam satellite networks.**

***Index Terms*—station-assisted multibeam satellite, utility maximization, cross-layer design, low-complexity**

I. Introduction

When disasters such as earthquakes, tsunamis, and hurricanes disrupt terrestrial network services, satellite networks can still support robust regional coverage for disaster recovery and rescue missions. The capability of satellites can be enhanced when they are interlinked with ground stations, which can fill coverage holes and improve system throughput. This "station-assisted" satellite network can perform better when the different types of components over the sky and on the ground are interconnected seamlessly by protocols and algorithms that consider the heterogeneity of the system [1].

One applicable scenario is the communications between a disaster recovery team when the team members are deployed in the area where terrestrial infrastructure is not available or heavily damaged [2], [3]. The recovery team sets up stations with mountable antennas that play a role of gateways and relay the satellite packets to end user terminals. Each end user terminal for a recovery team member may communicate via the stations or can directly receive the satellite signal. Given the multibeam capability with digital beamforming technology [4], the satellite can exploit path diversity, and the scheduler faces a problem of choosing a better signal route. The quality of service (QoS) requirements and priority of the packets should be taken into consideration as well. The path diversity can make the system performance less dependent on channel conditions, especially when some users are under a bad channel condition for a long time. Since the addition of ground stations changes not only physical layer channels but also the higher-layer decisions of routing and flow control, the principle of cross-layer optimization that spans from the Physical layer to the Transport layer should be applied for satellite-terrestrial network design. Though there have been many previous work on developing cross-layer schemes and improving existing protocols for space and aeronautical networks [5]–[7], we still need to fill a gap for interweaving satellites with terrestrial infrastructure by a good use of path diversity.

Recently, cross-layer solutions that can exploit wireless diversity in multi-hop ad-hoc networks have been studied [8]–[11]. A joint solution to the problem of congestion control and power control has also been developed [8]. Applying geometric programming technique to non-linearly constrained optimization, the solution has been shown to achieve optimal performance in a distributed manner. However, its application is limited and cannot be directly applied to satellite networks, where, as well as congestion control and power control, routing and scheduling under time-varying channels have to be addressed accordingly. Neely et al. has developed a joint solution to flow control, routing, and scheduling for heterogeneous networks [9]. Using the optimization techniques, they decouple flow control from routing and scheduling components while achieving optimal performance in networks with time-varying channels. The solution, however, does not take into account power control, which is commonly used in modern wireless systems to boost network capacity. Based on the result that signal fading in the satellite-Earth path can be predicted [12], [13], a joint solution to power allocation and routing has been developed [10]. Although the solution can achieve the largest stability region of arrival rates, it requires high computational complexity to find the power allocation and does not provide flow control, which makes it as an impractical and incomplete solution for satellite networks.

In this paper, we investigate the joint problem of power and traffic controls in the satellite-terrestrial heterogeneous networks under inter-beam interference. When the multibeam satellite has a choice of routing signals to ground stations (such as gateways, feeder antennas, or gap fillers) as well as sending directly to end user terminals, the users can benefit from the relaying through the ground stations, and at the same time, compete wireless resources with the stations due to the inter-beam interference. To this end, we answer to the questions that have not been addressed in the literature: how the users should share the station-assisted relay channels and how much power should be allocated to the shared channels. The problem

is challenging due to the cross-layer nature of the problem and the complex inter-beam interference relationship. We start with formal formulation of the joint utility maximization problem of flow control, routing, link rate control, and power control in the multi-beam satellite environment, and develop an optimal cross-layer solution under the inter-beam interference. In particular, we design the solution with per-link queues that simply the internal structure and make the solution amenable to implement.

This paper is organized as follows: In Section II, we formulate a cross-layer resource allocation problem for a satellite aided by ground stations. In Section III, multi-queue structure and algorithms for flow control, routing, link rate control, and power control are presented. In Section IV, the performance of the station-assisted satellite system is simulated. We conclude the paper in Section V.

II. System model

We consider a downlink satellite network that consists of multiple terminals (or users) and stations with a single satellite. In general, the stations can provide a larger capacity from higher antenna gain, and relay data from the satellite to the corresponding user. Each user can receive data relayed via associated stations, or directly from the satellite. The data relay from a station to a user is carried over ground wireless systems such as Long Term Evolution (LTE) or Wireless Local Area Network (WLAN), which are assumed to use separate frequency spectrum from the satellite networks and thus can transmit data without interfering with the satellite signals. The satellite can generate K different streams over a single frequency channel, and control transmission power of each stream using the-state-of-the-art phased array antenna made of gallium nitride (GaN) [14]. We also assume that time is slotted and the satellite can simultaneously transmit in one time slot up to K different streams to users or stations, which may interfere with each other if the receivers of different streams are closely located.

Let F denote the set of flows (or users) in the network, and let L denote the set of K difference beams (or streams/links). We define r_{fl} as data rate of flow $f \in F$ through satellite beam $l \in L$, and $\vec{r} := \{r_{fl}\}$ as its vector. When each beam l has transmission power $P_l(t)$ at time t, the capacity of stream l can be calculated using the Shannon capacity in the high signal-to-interference-plus-noise ratio (SINR) region with the received power from the Friis radio link formula [15], i.e.,

$$C_l(\vec{P}(t)) = \log_2 \frac{G_l^r G_l^t \left(\frac{\lambda}{4\pi L}\right)^2 \alpha_l^2(t) P_l(t)}{\sum_{k \neq l} G_l^r G_k^t \left(\frac{\lambda}{4\pi L}\right)^2 \alpha_l^2(t) H_{kl} P_k(t) + \eta}, \tag{1}$$

where $\vec{P}(t) := \{P_l(t)\}$, η denotes the additive white Gaussian noise (AWGN), G_l^t and G_l^r denote the transmitter and receiver antenna gain of stream l, respectively, λ is the carrier of wavelength, L is the altitude of the satellite, and α_l^2 accounts for weather-induced signal power attenuation (mainly from rain attenuation), which is assumed to be fixed within a single time slot but changes across time slots following a stationary distribution with finite states. H_{kl} denotes a factor of signal power leakage that takes into account interference from beam k to the receiver of stream l. In a conservative scenario of deploying the narrowest spotbeam illuminated by uniform planar transmission antenna with no interference suppression, the power leakage from the mainlobe of an adjacent beam is modeled as the 2-dimensional far-field Fourier transform of the transmission antenna distribution [16], [17]:

$$H_{kl} = \left(\text{sinc}\left(\frac{d_{kl}}{\lambda L/D}\right)\right)^2, \tag{2}$$

where $d_{kl} (< \frac{\lambda L}{D})$ denotes the distance between two receivers k and l, and D denotes the diameter of the transmission antenna. We assume a concave function for H within mainlobe beamwidth given by $\frac{\lambda L}{D}$. We also assume that total link capacity $\sum_l C_l(\vec{P}(t))$ is upper bounded by a constant R_{max} within the feasible region of $\vec{P}(t)$.

Let $U_f(R_f)$ denote utility of user f when user receives at rate R_f. The utility function should be increasing, strictly concave, and continuously differential. In this work, we particularly consider a logarithmic utility function $U_f(R_f) := w_f \log_2(R_f)$, where w_f is the weight of user f, since it often represents the priority of the user based on QoS level, service price, and so on. The logarithmic function has been widely used in the literature to achieve a proportional fair resource allocation [18]. Given the set L of selected K active beams, our objective is to find a solution $\vec{r}(t) = \{r_{fl}(t)\}$ of routing, flow control, and power allocation $\vec{P}(t)$ to the following utility maximization problem:

$$\text{maximize}_{\vec{r}(t),\vec{P}(t)} \quad \sum_{f \in F} U_f\left(\sum_{l \in L} r_{fl}(t)\right) \tag{3}$$

$$\text{subject to} \quad \sum_{f \in F} r_{fl}(t) \leq C_l(\vec{P}(t)),\ \forall\ l \tag{4}$$

$$\lim_{T \to \infty} \frac{1}{T} \sum_{t=0}^{T-1} \sum_{l \in L} P_l(t) \leq P_{avg}, \tag{5}$$

where the link flow sum is upper-bounded by the Shannon capacity, and the total power is constrained by P_{avg} in average with back-off of power amplifiers into consideration, to ensure linearity in the operating region.We assume that the maximum total power constraint P_{tot} is sufficiently greater than P_{avg}. Later in Section IV, we relax the assumption and apply strict power constraints under which the power sum should be no greater than the total power constraint P_{tot} *at each time* t. We show through simulations that (5) can be still applied after normalization without losing the performance.

III. Station-Assisted Traffic Control

Inspired by the routing approach in [10], we develop on-board multi-queue structure, which consists of flow queues, flow-link queues, and link queues in the satellite, as shown in Fig. 1. The overall procedure is as follows.

- At each time t, each flow f injects $R_f(t) \leq (M+1)R_{max}$ packets to flow queue $Q_f(t)$, where $M := K - |F|$ denotes the number of stations and $|\cdot|$ denotes the cardinality.

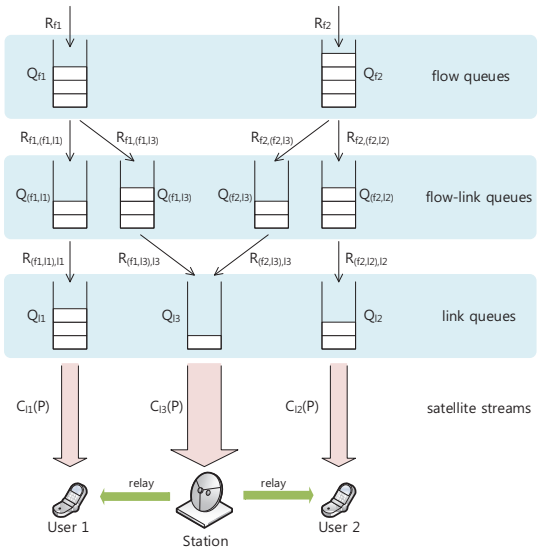

Fig. 1. Satellite on-board multi-queue structure with relay stations.

- $R_{fv}(t)$ packets move from flow queue $Q_f(t)$ to flow-link queue $Q_v(t)$, where $v := (f, l)$ is a pair of flow f and link stream l. To prevent sudden queue increase, we restrict $R_{fv}(t) \leq R_{max}$.
- $R_{vl}(t) \leq R_{max}$ packets move from flow-link queue $Q_v(t)$ to link queue $Q_l(t)$. We restrict $\sum_v R_{vl}(t) \leq R_{max}$ for each l.
- $C_l(\vec{P}(t))$ packets from $Q_l(t)$ are transmitted over link stream l.
- The power consumption is measured by power queue $Q_p(t)$.
- Each queue evolves as

$$\begin{aligned} Q_f(t+1) &= (Q_f(t) - \textstyle\sum_v R_{fv}(t))^+ + R_f(t), \\ Q_v(t+1) &= (Q_v(t) - R_{vl}(t))^+ + R_{fv}(t), \\ Q_l(t+1) &= \left(Q_l(t) - C_l(\vec{P}(t))\right)^+ + \textstyle\sum_v R_{vl}(t), \\ Q_p(t+1) &= Q_p(t) + \beta(\textstyle\sum_l \vec{P}_l(t) - P_{avg}), \end{aligned} \tag{6}$$

where $(\cdot)^+ := \max\{0, \cdot\}$ and $\beta > 0$ is a small step size.

We claim that the above bounds on R_f, R_{fv}, and R_{vl} do not reduce the maximum system performance since the total link capacity $\sum_l C_l(\vec{P}(t))$ is upper bounded by R_{max}. The detailed proof is provided in Appendix A.

In our system architecture, we use the Lyapunov technique to develop an optimal solution. We investigate certain properties such that if a solution satisfies some conditions related to the Lyapunov drift, it can achieve the optimal performance. To this end, we first consider a static near-optimal solution $\{\bar{R}_f^*, \bar{R}_{fv}^*, \bar{R}_{vl}^*, \bar{P}_l^*\}$ to (3) with the following additional constraints: for a given $\epsilon > 0$,

$$\begin{aligned} \bar{R}_f^* &\leq \textstyle\sum_v \bar{R}_{fv}^* - \epsilon \\ \bar{R}_{fv}^* &\leq \bar{R}_{vl}^* - \epsilon \\ \textstyle\sum_v \bar{R}_{vl}^* &\leq C_l(\bar{P}^*) - \epsilon \\ \textstyle\sum_l \bar{P}_l^* &\leq P_{avg} - \epsilon. \end{aligned} \tag{7}$$

Since the constraints enforce the system stability, it is clear that $\{\bar{R}_f^*, \bar{R}_{fv}^*, \bar{R}_{vl}^*, \bar{P}_l^*\}$ is a near-optimal solution such that, as $\epsilon \to 0$,

$$\sum_f U_f(\bar{R}_f^*) \to \sum_f U_f(R_f^*), \tag{8}$$

where $\{R_f^*, R_{fv}^*, R_{vl}^*, P_l^*\}$ is an optimal solution to (3).

We define a Lyapunov function $\mathcal{L}(t)$ as

$$\mathcal{L}(t) := \sum_f Q_f(t)^2 + \sum_v Q_v(t)^2 + \sum_l Q_l(t)^2 + \frac{1}{\beta} Q_p(t)^2.$$

Since $R_f(t)$ is upper bounded, there is U_{max} such that $U_f(R_f(t)) \leq U_{max}$. Note that the data queues denote the demand for transmissions, while the power queues $Q_p(t)$ are introduced to avoid excessive power consumption of the links. Our control will result in scheduling the links with high data queue and low power queue. The following lemma follows the same line of analysis as in [9].

Lemma 1: Suppose that the following inequality holds,

$$\begin{aligned} &\Delta(Q(t)) := E\left[\mathcal{L}(t+1) - \mathcal{L}(t) \mid Q(t)\right] \\ &\leq B - \epsilon \left(\textstyle\sum_f Q_f(t) + \sum_v Q_v(t) + \sum_l Q_l(t) + Q_p(t)\right) \\ &\quad - V \textstyle\sum_f U_f(\bar{R}_f^*) + V \sum_f E[U_f(R_f(t)) \mid Q(t)], \end{aligned} \tag{9}$$

for some constant B, V, and $\epsilon > 0$, and $Q(t) := \{Q_f(t), Q_v(t), Q_l(t), Q_p(t)\}$. Then we have that

$$\lim_{T\to\infty} \frac{1}{T} \sum_{t=0}^{T-1} \left(\textstyle\sum_f Q_f(t) + \sum_v Q_v(t) + \sum_l Q_l(t) + Q_p(t)\right) \leq \frac{B + V|F|U_{max}}{\epsilon}, \tag{10}$$

$$\sum_f U_f\left(\lim_{T\to\infty} \frac{1}{T} \sum_{t=0}^{T-1} R_f(t)\right) \geq \sum_f U_f(\bar{R}_f^*) - \frac{B}{V}. \tag{11}$$

Remark: The parameter V is a tunable system parameter that weighs the utility with respect to the stability, and its configuration is often left to the operators (see for example in [9]). A higher value of V implies that the operators relatively weigh the utility than the stability, and the system will be stabilized at higher queue lengths. On the other hand, by reducing the value of V, the system will keep the queue lengths low and thus can converge quickly at the expense of the utility loss. We will show throughput simulations the impact of V on the performance in Section IV.

Lemma 1 implies that if (9) is always true for sufficiently large queue lengths, the system will be stabilized (by (10)) and achieve the performance arbitrarily close to the optimal utility (by (11)), i.e., a scheme with (9) is an optimal solution to (3). The detailed proof is provided in Appendix B.

We now claim that the following set of algorithms satisfy (9).

- **Flow control:** set $R_f(t) = r_f$, which is a solution to

$$\begin{aligned} &\text{maximize} \quad \textstyle\sum_f V U_f(r_f) - 2Q_f(t) r_f \\ &\text{subject to} \quad r_f \leq (M+1) R_{max} \text{ for all } f. \end{aligned} \tag{12}$$

From the concavity of $U_f(\cdot)$, we can solve $VU_f'(r_f) - 2Q_f(t) = 0$ independently for each flow f. The parameter V can be interpreted as a weighting factor for the utility.

- **Routing:** set $R_{fv}(t) = r_{fv}$, which is a solution to

$$\begin{array}{ll} \text{maximize} & \sum_f \sum_{v:(f,l')} (Q_f(t) - Q_v(t)) r_{fv} \\ \text{subject to} & r_{fv} \le R_{max} \text{ for all } f, v. \end{array} \tag{13}$$

It can be easily shown that this solution is, for each f, $R_{fv}(t) = R_{max}$ for v such that $Q_v(t) < Q_f(t)$, and $R_{fv}(t) = 0$ otherwise. In other words, R_{max} packets move from $Q_f(t)$ to any queue $Q_v(t) < Q_f(t)$.

- **Link rate control:** set $R_{vl}(t) = r_{vl}$, which is a solution to

$$\begin{array}{ll} \text{maximize} & \sum_{v:(f',l)} \sum_l (Q_v(t) - Q_l(t)) r_{vl} \\ \text{subject to} & \sum_{v:(f',l)} r_{vl} \le R_{max} \text{ for all } l. \end{array} \tag{14}$$

Similarly, for each l, we will have $R_{vl}(t) = R_{max}$ if $v = \text{argmax}_{v':(f',l)} Q_{v'}(t)$ with In other words, R_{max} packets move to $Q_l(t)$ from the longest queue $Q_v(t) > Q_l(t)$.

- **Power allocation:** for small $\epsilon_1 > 0$, find $\vec{P}(t)$ within $\frac{\epsilon_1}{2}$ from the maximum of

$$\sum_l Q_l(t) C_l(\vec{P}(t)) - Q_p(t) P_l(t) \tag{15}$$

subject to $P_l \le P_{tot}$ for all l.

To show that the above solution satisfies (9), we start with the Lyapunov drift $\Delta(Q(t))$. We drop t when there is no confusion.

$$\begin{aligned} &\Delta(Q(t)) := E\left[\mathcal{L}(t+1) - \mathcal{L}(t) | Q(t)\right] \\ &\le B' + 2\sum_f Q_f E[R_f - \textstyle\sum_{v:(f,l')} R_{fv} | Q] \\ &\quad + 2\textstyle\sum_{v:(f,l)} Q_v E[R_{fv} - R_{vl} | Q] \\ &\quad + 2\textstyle\sum_l Q_l E[\sum_{v:(f',l)} R_{vl} - C_l(\vec{P}) | Q] \\ &\quad + 2Q_p E[\textstyle\sum_l P_l - P_{avg} | Q] \\ &\le B' + 2\textstyle\sum_f Q_f E[R_f | Q] - 2\sum_f \sum_l (Q_f - Q_v) E[R_{fv} | Q] \\ &\quad - 2\textstyle\sum_f \sum_l (Q_v - Q_l) E[R_{vl} | Q] \\ &\quad - 2\textstyle\sum_l E[Q_l C_l(\vec{P}) - Q_p P_l | Q] - Q_p P_{avg}, \end{aligned} \tag{16}$$

where $B' := (|F|+1)(K+1)R_{max}^2 + |K| P_{tot}^2$. The second inequality holds because $\sum_{v:(f,l')}$, $\sum_{v:(f',l)}$, $\sum_{v:(f,l)}$ can be written as $\sum_l$, $\sum_f$, $\sum_f \sum_l$, respectively, by setting $R_{fv} = 0$ and $R_{vl} = 0$ for non-existing paths.

Now we define

$$\Psi(Q(t)) := \textstyle\sum_f E\left[VU_f(R_f) - 2Q_f R_f | Q\right], \tag{17}$$

$$\begin{aligned} \Phi(Q(t)) &:= 2\textstyle\sum_f \sum_l (Q_f - Q_v) E[R_{fv} | Q] \\ &\quad + 2\textstyle\sum_f \sum_l (Q_v - Q_l) E[R_{vl} | Q], \end{aligned} \tag{18}$$

$$\Theta(Q(t)) := 2\textstyle\sum_l E[Q_l C_l(\vec{P}) - Q_p P_l | Q]. \tag{19}$$

Then from (16), we have that

$$\begin{aligned} \Delta(Q(t)) \le B' &- \Phi(Q(t)) - \Theta(Q(t)) - \Psi(Q(t)) - Q_p(t) P_{avg} \\ &+ V\textstyle\sum_f E[U_f(R_f(t)) | Q]. \end{aligned}$$

Since our algorithms search in a larger space than the near-optimal solution $\{\bar{R}_f^*, \bar{R}_{fv}^*, \bar{R}_{vl}^*, \bar{P}^*\}$, we can obtain that, from our flow control (12),

$$\Psi(Q(t)) \ge V\textstyle\sum_f U_f(\bar{R}_f^*) - 2\sum_f Q_f \bar{R}_f^*. \tag{20}$$

Similarly, from our routing (13) and link rate control (14), we have that

$$\Phi(Q(t)) \ge 2\textstyle\sum_f \sum_l (Q_f - Q_v) \bar{R}_{fv}^* + 2\sum_f \sum_l (Q_v - Q_l) \bar{R}_{vl}^*, \tag{21}$$

and from our power allocation (15),

$$\Theta(Q(t)) \ge 2\textstyle\sum_l \left(Q_l C_l(\bar{P}^*) - Q_p \bar{P}_l^*\right) - \epsilon_1. \tag{22}$$

Combining (20)-(22) with (7), we can obtain that

$$\begin{aligned} &\Delta(Q(t)) \\ &\le B' + 2\textstyle\sum_f Q_f \bar{R}_f^* - 2\sum_f \sum_l (Q_f - Q_v) \bar{R}_{fv}^* \\ &\quad - 2\textstyle\sum_f \sum_l (Q_v - Q_l) \bar{R}_{vl}^* - 2\sum_l \left(Q_l C_l(\bar{P}^*) - Q_p \bar{P}_l^*\right) + \epsilon_1 \\ &\quad - V\textstyle\sum_f U_f(\bar{R}_f^*) - Q_p(t) P_{avg} + V\sum_f E[U_f(R_f(t)) | Q] \\ &\le B + 2\textstyle\sum_f Q_f(\bar{R}_f^* - \sum_v \bar{R}_{fv}^*) + 2\sum_v Q_v(\bar{R}_{fv}^* - \bar{R}_{vl}^*) \\ &\quad + 2\textstyle\sum_l Q_l(\sum_v \bar{R}_{vl}^* - C_l(\bar{P}^*)) + 2Q_p(\sum_l \bar{P}_l^* - P_{avg}) \\ &\quad - V\textstyle\sum_f U_f(\bar{R}_f^*) + V\sum_f E[U_f(R_f(t)) | Q] \\ &\le B - 2\epsilon \left(\textstyle\sum_f Q_f(t) + \sum_v Q_v(t) + \sum_l Q_l(t) + Q_p(t)\right) \\ &\quad - V\textstyle\sum_f U_f(\bar{R}_f^*) + V\sum_f E[U_f(R_f(t)) | Q], \end{aligned} \tag{23}$$

where $B := B' + \epsilon_1$. The inequalities hold at each time t, and therefore, from Lemma 1, our solution (12)-(15) achieves the utility sum that is arbitrarily close to the maximum.

Remarks: Power allocation (15) operates with per-link queues and does not require per-flow queues as in conventional optimal schedulers [9], [10], which significantly simplifies the internal buffer structure [19].

Note that (20) and (21) can be solved easily from the proposed flow control (12), routing (13), and link rate control (14) schemes. However, the solution to (15) cannot be easily obtained since it is a non-convex problem over an uncountable set of feasible power allocations. Motivated by [8], we convert the problem to a convex form and obtain the solution through an iterative method.

Let $X_l := \log_2 P_l$. We can formulate an optimization problem equivalent to (15):

$$\begin{array}{ll} \max\limits_{\vec{X}} & \sum\limits_l \left(Q_l C_l(2^{\vec{X}}) - Q_p 2^{X_l}\right) \\ \text{subject to} & 2^{X_l} \le P_{tot} \text{ for all } l. \end{array} \tag{24}$$

Each term $(Q_l C_l - Q_p 2^{X_l})$ in (24) indicates the difference between the potential performance gain $(Q_l C_l)$ and the power penalty $(Q_p 2^{X_l})$ of link l under the power allocation $\vec{X}$. From our definition, Q_p can be interpreted as a weighting factor for power consumption $P_l (= 2^{X_l})$ of user l.

From (1), the problem can be re-written as

$$\max_{\vec{X}} \sum_l \Big(Q_l (\log_2 G_l^r G_l^t \left(\frac{\lambda}{4\pi L}\right)^2 \alpha_l^2 + X_l) - Q_l \log_2 (\sum_{k\neq l} G_l^r G_k^t \left(\frac{\lambda}{4\pi L}\right)^2 \alpha_l^2 H_{kl} 2^{X_k} + \eta) - Q_p 2^{X_l} \Big)$$
sub. to $X_l \leq \log_2 P_{tot}$ for all l, (25)

which is clearly a convex problem, and can be solved using the following iterative method:

$$X_l(i+1) = \min \Big\{ \log_2 P_{tot}, \quad X_l(i) + \kappa \Big(Q_l - Q_p 2^{X_l(i)} - \sum_{k\neq l} Q_k \frac{G_k^r G_l^t \left(\frac{\lambda}{4\pi L}\right)^2 \alpha_k^2 H_{kl} 2^{X_l(i)}}{\sum_{j\neq k} G_k^r G_j^t \left(\frac{\lambda}{4\pi L}\right)^2 \alpha_k^2 H_{jk} 2^{X_j(i)} + \eta} \Big) \Big\}, \tag{26}$$

where $\kappa > 0$ is a small step size in the dB scale. The iteration stops when $\sum_l |X_l(i+1) - X_l(i)| \leq \delta$ where $\delta \leq \frac{\kappa}{K \log_2 P_{tot}} \cdot \frac{\epsilon_1}{2}$. Suppose that the iteration terminates after i-th run. We set $P_l^{\#} = 2^{X_l(i)}$. Given $Q(t)$, let $g(\vec{P}) := \sum_l (Q_l C_l(\vec{P}) - Q_p P_l)$. Suppose that the maximum of $g(\vec{P})$ can be attained at $\vec{P}^*$, and let $X_l^* := \log_2 P_l^*$. From the concavity of $g(e^{\vec{X}})$, we can obtain that

$$\begin{aligned} |g(\vec{P}^{\#}) - g(\vec{P}^*)| &= |g(2^{\vec{X}(i)}) - g(2^{\vec{X}^*})| \\ &\leq |\nabla g(2^{\vec{X}(i)})^T (\vec{X}(i) - \vec{X}^*)| \\ &\leq K \cdot \frac{\delta}{\kappa} \cdot \log_2 P_{tot} \leq \frac{\epsilon_1}{2}, \end{aligned} \tag{27}$$

and thus (22) holds. The power allocation to link l would increase with high Q_l and, decrease with high Q_p and high interference to its neighboring links. The computation of (26) can be obtained without difficulty, assuming that the satellite has the location information of all users and stations, and can predict the channel state of each beam with high probability [12], [13].

In summary, we have developed an optimal cross-layer solution that maximizes total utility by using the Lyapunov technique. Combining (12), (13), (14), and (26) with queue evolution (6), our solution of flow control, routing, link rate control, and power control is shown to be provably efficient and amenable to implement in practice with simplified queue structure. We emphasize that the controls of link rate and power allocation that maximize the capacity is often an NP-Hard problem due to the non-linear, non-convex interference relation between multiple beams [20], and in the previous works, the difficulty is avoided by assuming no interference [10] or by ignoring the scheduling problem [8]. Finally, we note that Eqs. (6), (12)-(14) can be obtained in a closed form with $O(1)$ complexity at each time. In our solution, we replace (15) with (26), which can be obtained using an iterative method.

In the following, we evaluate our proposed scheme through simulations with practical satellite system configuration.

TABLE I
CONFIGURATION

Max power P_{tot}	1000 Watts
Target power P_{avg}	500 Watts
Beamwidth	50 Km
Frequency (wavelength)	20 GHz (0.015 m)
(Base) Bandwidth	10 MHz
Noise power	$4 \cdot 10^{-15}$ per Hz
Satellite altitude	$3.58 \cdot 10^4$ km
Satellite Tx antenna diameter	10 m
User Rx antenna diameter	0.1 m
Station Rx antenna diameter	$0.1 \sim 1$ m
κ	0.0001
β	0.1
V	10^4
R_{max}	50 packets

IV. SIMULATIONS

This section provides simulation results and compares our schemes with and without power control. Without power control, we allocate an identical amount of power to each stream by evenly dividing P_{avg}. The satellite at altitude 3.58×10^4 km provides communication service using 20 GHz frequency and can support multiple beams simultaneously, with each narrow beamwidth of 50 km. Detailed configuration is provided in Table I. In our setting, the antenna gains of the transmitter and the receivers can be obtained as $G^t = \frac{4\pi A_e^t}{\lambda^2} = \left(\frac{\pi D}{\lambda}\right)^2$ and $G^r = \frac{4\pi A_e^r}{\lambda^2} = \left(\frac{\pi d}{\lambda}\right)^2$, where the effective antenna areas of A_e^t for transmitter and A_e^r for receiver are assumed to be equal to the actual antenna size of transmission antenna diameter D and reception antenna diameter d. Time is slotted with length of 10 ms, and the packet size is fixed to 1000 bytes. We assume the identical user weight $w_f = 1$ for all the users for simplicity.

We first consider a network with 20 active user and M stations for $M \in \{0, 1, 2, 3, 4, 5\}$ in square-shaped areas. All the users and stations are assumed in the three equally likely channel states of light, moderate, and heavy attenuation, with Markov transition probability 0.1, between light and moderate, and between moderate and heavy, as shown in Fig. 2. The attenuation of each user/station is modeled as an independent and identically distributed (i.i.d.) lognormally Gaussian random process with mean and standard deviation pairs of $(-ln(1.23), \sqrt{0.014}), (-ln(2.27), \sqrt{0.014})$, and $(-ln(4.0), \sqrt{0.077})$ for light, moderate, and heavy, respectively [13]. We change the square area from 200×200 km^2 to 1000×1000 km^2. As the area expands, the network becomes sparse and the inter-beam interference becomes less severe. To see the impact of alternative paths through stations, we set the antenna diameter of the stations to 0.1 m as the users. The power control is used by default unless specified.

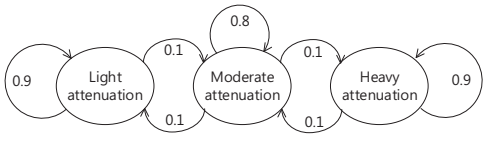

Fig. 2. Markovian channel state transition.

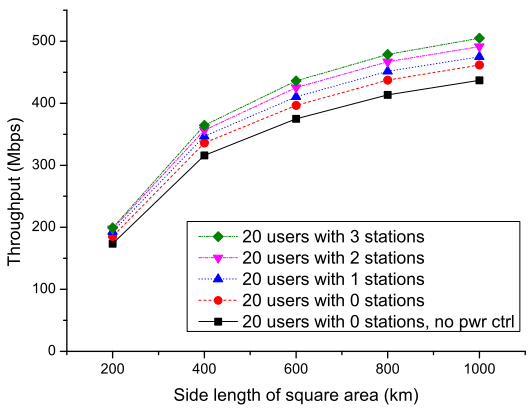

(a) Throughput

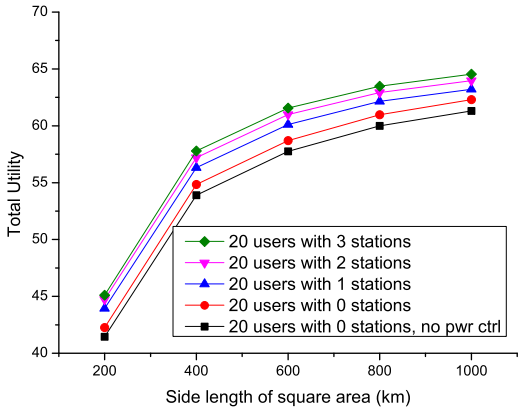

(b) Total utility

Fig. 3. Performance gains from alternative paths through additional stations and power control under various user densities.

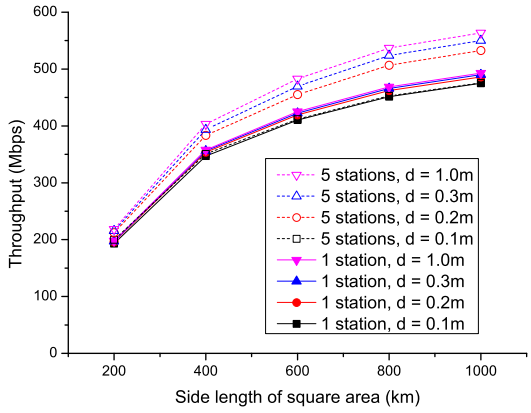

Fig. 4. The impact of antenna gains is not significant than the number of stations; different receiver antenna diameter d for $K = 21$ with 1 and 5 station(s).

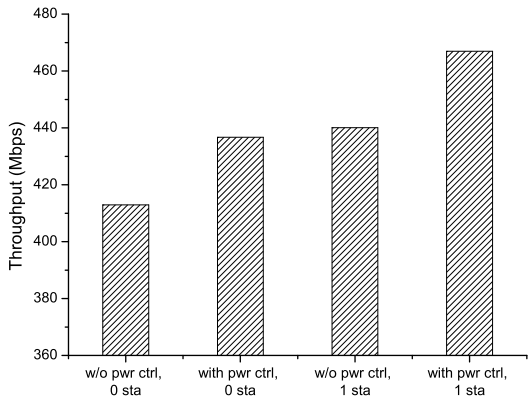

Fig. 5. Throughput performance of 20 users in 800×800 km^2 square area. The gains of the alternative path through the station and the power control are stackable.

We randomly create 10 topologies with 25 nodes, and for each topology, 20 nodes represent the users, and the rest nodes are either a station or abandoned, depending on how many stations we are using. For each scenario, we run simulations 10 times with different traffic instances. Each point in Fig. 3 represents their average over 100 simulation runs. The scheme without station nor power control serves as the basis for the others. The results show that alternative paths through stations as well as the use of power control can improve the throughput and utility significantly, and the sparser the network is, the higher performance gains are achieved. The power control contributes to mitigate inter-beam interference, and the alternative paths through stations provide additional opportunity to the users to receive data, in particular, when the stations have good channel condition and experience less inter-beam interference.

Fig. 4 shows the impact of the antenna gains of the stations. We fix the number of users to 20 and the number of stations to 1 or 5 and have changed the antenna diameter of the station between $0.1 \sim 1$ m. The results show that the performance improves as the antenna diameter increases. However, the differences are not much significant, since the antenna gain scales both the desired signal and interferences in the same way and the signal gain from the larger antenna diameter is offset by the severer inter-beam interference.

Fig. 5 provides a closer view for performance gain of the power control and the station in networks with 20 users (and 0 or 1 station) deployed in 800×800 km^2 square area (average over 10 different topologies). In this experiment (and in the sequel), we set the antenna diameter of the station to 0.3 m. The results show that the power control improves the throughput by $5.7 \sim 6.1$ % and the station provides the gain of $6.6 \sim 6.9$ %. Interestingly, it shows that the gains of the power control and the alternative path through the station are stackable. The reason will be further explained in the following.

Fig. 6 illustrates the throughput achieved at each user in a network with 20 users (and with 0 or 1 station) deployed in 800×800 km^2 square area. We also compare the performance with and without the power control. From the individual

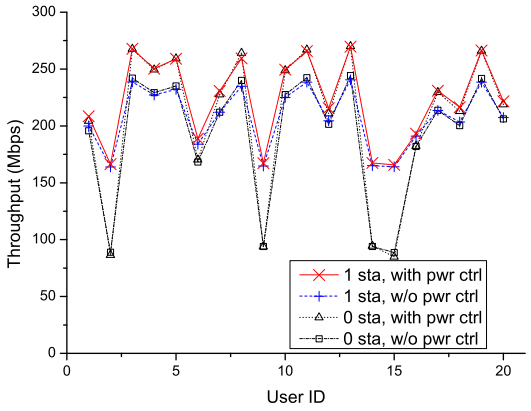

Fig. 6. Performance of 20 users in 800×800 km^2 square area. The alternative path through station improves the fairness and the power control leads to higher throughput performance.

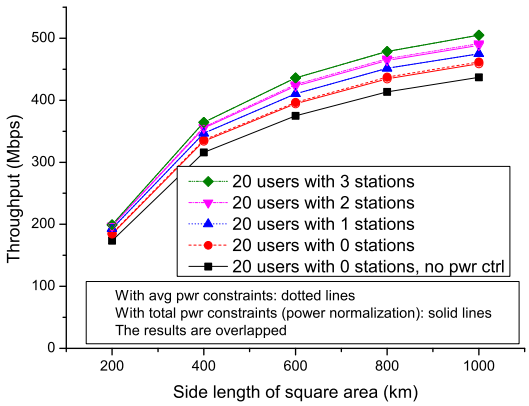

Fig. 7. Performance of the normalized power allocation under the strict power constraints and the original solution under the average power constraint. They are almost coincident.

user's performance, we calculate the Jain's fairness index $\mathcal{I} = \frac{(\sum_n x_n)^2}{20\cdot\sum_n x_n^2}$, where x_n denotes the throughput of user n [21]. As the index is close to 1, the users achieve similar throughput. The results in Table II show that the additional station significantly improves the fair resource sharing by giving to low-throughput users another path to exploit. The power control seems to harm the fairness. However, a closer examination of Fig. 6 reveals that the power control improves the performance of the users with high throughput (i.e., users of ID 3, 4, 5, 8, 10, 11, 13, 17, 19) without harming the performance of the users with low throughput (i.e., users of ID 2, 9, 14, 15), and thus results in a slightly low fairness index. It is an interesting observation that the additional stations are helpful to the low-throughput users, and the power control is effective in the performance improvement of the high-throughput users. This also explains why the performance gains from the station-assisted path and the power control are stackable.

TABLE II
JAIN'S FAIRNESS INDEX.

0 sta, w/o pwr ctrl	0.9257
0 sta, with pwr ctrl	0.9113
1 sta, w/o pwr ctrl	0.9818
1 sta, with pwr ctrl	0.9719

In the next simulation, we replace the average power constraints (5) with strict power constraints. To elaborate, we require $\sum_{l\in L} P_l(t) \le P_{tot}$ at each time t (and thus the assumption of $P_{avg} \ll P_{tot}$ is removed). Note that since the scheduling problem under the conflict graph is NP-Hard in general [20], our problem under the strict power constraints is also NP-Hard. We approximate the optimal solution using our results, i.e., we utilize $P_l(t) = 2^{X_l^*}$ where X_l^* is obtained from the iterative method (26) by replacing P_{avg} with P_{tot}. Note that $P_l(t)$ may not be feasible under the new power constraints, since the solution is obtained from the average power constraints. In such case, we obtain a feasible solution $\{\tilde{P}_l(t)\}$ by normalizing $\{P_l(t)\}$ as

$$\tilde{P}_l(t) = \begin{cases} P_l(t) & \text{if } \sum_l P_l(t) \le P_{tot}, \\ P_l(t)P_{tot}/(\sum_l P_l(t)) & \text{otherwise.} \end{cases}$$

Fig. 7 shows the results of our solution with the strict power constraints and the average power constraints in the same system environment as in Fig. 3. We can observe that they are almost coincident.

Fig. 8 shows the impact of parameter V. As we increase the value of V, our proposed solution achieves a higher throughput (Fig. 8(a)). However, the performance gains come with larger delays (Fig. 8(b)), since the large average queue lengths imply poor delay performance. We note that our solution is relatively insensitive to the value of V, and a large range $[10^4, 10^5]$ of V leads to good performance. Also, as shown in our analysis, the parameter V provides a tradeoff between the utility and the system stability.

V. CONCLUSION

We develop a cross-layer resource allocation in station-assisted satellite networks under inter-beam interference. Jointly takeing into consideration of flow control, routing, link rate control, and power control, our solution improves the spectrum efficiency, by exploiting the path diversity through the ground station(s), and by orchestrating the multibeam power under the inter-beam interference. We design the solution with a simplified queue structure, which facilitates practical implementation.

We formulate the network utility optimization problem, and analytically show that our cross-layer solution achieves the optimal performance under time-varying channel conditions and inter-beam interference. Simulation results demonstrate that the use of ground stations increase the performance of the multibeam satellite, in particular, for low-throughput users, and the adaptive power control enhances the performance of high-throughput users, without affecting the others.

For future work, uplink scheduling can be incorporated with our downlink solution for the coexistence case of uplink and

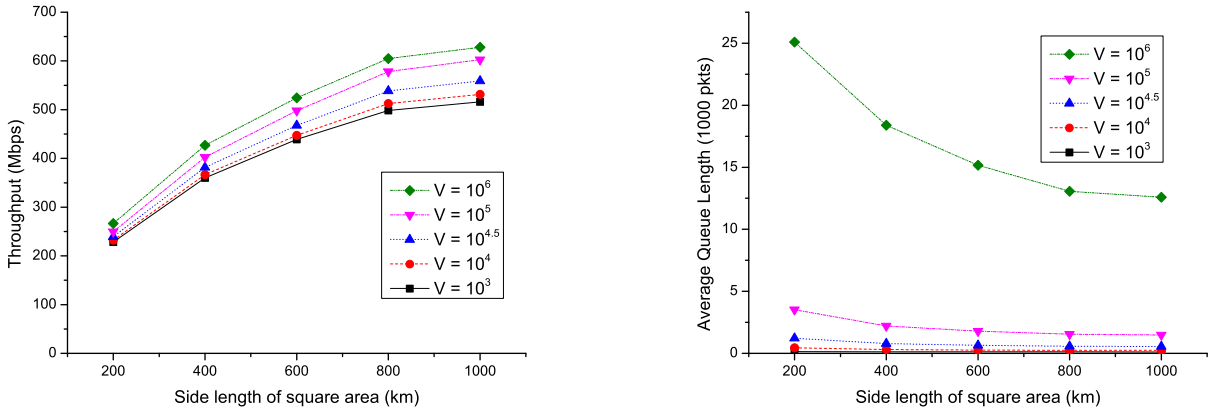

(a) Throughput

(b) Average queue length

Fig. 8. A larger V leads to better throughput at the expense of larger queue lengths, which imply higher packet delays.

downlink. In addition, as our results motivate the efficient use of station-assisted satellite networks, it is widely open to come up with end-to-end coordination of the satellite network and the ground networks by taking into account practical QoS constraints, e.g., average packet delay.

ACKNOWLEDGMENT

This research was supported in part by Basic Science Research Program through the National Research Foundation of Korea (NRF) funded by the Ministry of Science, ICT & Future Planning (No. NRF-2014R1A1A1A05002557) and in part by the Daegu Gyeongbuk Institute of Science and Technology through the MIREBraiN program.

REFERENCES

[1] S. Kota, G. Giambene, and S. Kim, "Satellite Component of NGN: Integrated and Hybrid Networks," *Int. Journal of Satellite Comm. and Networking*, vol. 29, pp. 191-208, 2011.

[2] M. Berioli, A. Molinaro, S. Morosi and S. Scalise, "Aerospace Communications for Emergency Applications," *Proceedings of the IEEE*, vol. 99, no. 11, pp. 1922-1938, Nov. 2011.

[3] Report ITU-R M.2149-1, "Use and Examples of Mobile-Satellite Service Systems for Relief Operation in the Event of Natural Disasters and Similar Emergencies," M Series, Mobile, Radiodetermination, Amateur and Releated Satellite Services, Oct. 2011.

[4] W. Li, X. Huang and H. Leung, "Performance Evaluation of Digital Beamforming Strategies for Satellite Communications," *IEEE Transactions on Aerospace and Electronic Systems*, vol. 40, no. 1, Jan. 2004.

[5] T. De Cola and M. Marchese, "Performance Analysis of Data Transfer Protocols over Space Communications," *IEEE Transactions on Aerospace and Electronic Systems*, vol. 41, no. 4, Oct. 2005.

[6] R. Wang, B. Gutha and P. V. Rapet, "Window-Based and Rate-Based Transmission Control Mechanisms over Space-Internet Links," *IEEE Transactions on Aerospace and Electronic Systems*, vol. 44, no. 1, Jan. 2008.

[7] J. P. Rohrer, *et. al.*, "Highly-Dynamic Cross-Layered Aeronautical Network Architecture," *IEEE Transactions on Aerospace and Electronic Systems*, vol. 47, no. 4, Oct. 2011.

[8] M. Chiang, "To Layer or Not To Layer: Balancing Transport and Physical Layers in Wireless Multihop Networks," in *IEEE INFOCOM 2004*, pp. 2525–2536, March 2004.

[9] M. J. Neely, E. Modiano, and L. Chih-Ping, "Fairness and Optimal Stochastic Control for Heterogeneous Networks," in *IEEE INFOCOM 2005*, pp. 1723–1734, March 2005.

[10] M. J. Neely, E. Modiano, and C. E. Rohrs, "Power Allocation and Routing in Multibeam Satellites with Time-varying Channels," *IEEE/ACM Trans. Netw.*, vol. 11, no. 1, pp. 138–152, 2003.

[11] J. Choi, W. Pak, and C. Joo, "Utility Maximization for Arbitrary Traffic in Communication Networks," *IEEE Communications Letters*, vol. 16, no. 10, pp. 1715–1718, Oct. 2012.

[12] J. P. Choi and V. W. S. Chan, "Predicting and Adapting Satellite Channels with Weather-Induced Impairments," *IEEE Transactions on Aerospace and Electronic Systems*, vol. 38, no. 3, July 2002.

[13] J. P. Choi, "Channel Prediction and Adaptation over Satellite Channels with Weather-Induced Impairments," Masters Thesis, EECS, MIT, May 2000.

[14] U. K. Mishra, P. Parikh, and Y.-F. Wu, "AlGaN/GaN HEMTs - An Overview of Device Operation and Applications," *Proceedings of the IEEE*, vol. 90, no. 6, pp. 1022-1031, June 2002.

[15] D. M. Pozar, *Microwave Engineering*, 4th ed., Wiley, 2011.

[16] J. Goodman, *Introduction to Fourier Optics*, 3rd ed. Roberts & Company, 2005.

[17] J. P. Choi and V. W. S. Chan, "Resource Management for Advanced Transmission Antenna Satellites," *IEEE Trans. on Wireless Communications*, vol. 8, no. 3, pp. 1308-1321, March 2009.

[18] F. R. Kelly, A. K, Maulloo, and D. K. H. Tan, Rate control for communication networks: shadow prices, proportional fairness and stability, *Journal of the Operational Research Society*, vol. 49, pp. 237-252, 1998.

[19] B. Ji, C. Joo, and N. B. Shroff, "Throughput-Optimal Scheduling in Multihop Wireless Networks Without Per-Flow Information," *IEEE/ACM Trans. on Networking*, vol. 21, no. 2, pp. 634–647, April 2013.

[20] C. Joo, G. Sharma, N. B. Shroff and R. R. Mazumdar, On the Complexity of Scheduling in Wireless Networks, *EURASIP Journal on Wireless Communications and Networking*, Oct. 2010.

[21] R. Jain, D. M. Chiu, and W. Hawe, "A Quantitative Measure of Fairness and Discrimination for Resource Allocation in Shared Computer Systems," *DEC Research Report*, 1984.

APPENDIX

A. Proof of achieving maximum system performance with bounds on R_f, R_{fv}, and R_{vl}

We show that the bounds of $R_f \leq (M+1)R_{max}, R_{fv} \leq R_{max}$, and $\sum_v R_{vl} \leq R_{max}$ do not reduce the maximum system performance. Let r^*_{fl} denote a static optimal solution to the original problem. Then there exist an static optimal solution $R^*_f, R^*_{fv}, R^*_{vl}$ that satisfies $r^*_{fl} \leq R^*_{fv} \leq R^*_{vl}$ and $\sum_l r^*_{fl} \leq R^*_f$ from our construction of the multi-queue structure.

Since $C_l(\cdot) < R_{max}$ for all l, we have $\sum_f r^*_{fl} \leq R_{max}$ for all l, $r^*_{fl} < R_{max}$ for all f, l, and $\sum_l r^*_{fl} < (M+1)R_{max}$,

where $M = K - |F|$ denotes the number of stations. Then we can also find a static optimal solution that satisfies $\sum_v R^*_{vl} \leq R_{max}$, $R^*_{fv} \leq R^*_{vl} < R_{max}$, and $R^*_f < (M+1)R_{max}$. This implies that the bounds on R_f, R_{fv}, and R_{vl} do not exclude the static optimal solution and hence, the maximum system performance will be achieved. ■

B. Proof of Lemma 1

Eq. (9) holds for all time t. Taking expectations over $Q(t)$ and summing up over $t \in [0, T-1]$, we obtain that

$$\begin{aligned} &E\left[\mathcal{L}(T) - \mathcal{L}(0)\right] \leq BT \\ &- \epsilon \sum_{t=0}^{T-1} E\left[\sum_f Q_f(t) + \sum_v Q_v(t) + \sum_l Q_l(t) + Q_p(t)\right] \\ &- VT \sum_f U_f(\bar{R}^*_f) + V \sum_{t=0}^{T-1} \sum_f E[U_f(R_f(t))]. \end{aligned} \tag{28}$$

From $\mathcal{L}(T) \geq 0$ and $U_f(\bar{R}^*_f) \geq 0$, we have that

$$\begin{aligned} &\epsilon \sum_{t=0}^{T-1} E\left[\sum_f Q_f(t) + \sum_v Q_v(t) + \sum_l Q_l(t) + Q_p(t)\right] \\ &\qquad \leq E[\mathcal{L}(0)] + BT + V \sum_{t=0}^{T-1} \sum_f E[U_f(R_f(t))]. \end{aligned} \tag{29}$$

From the boundedness of $R_f(t)$, there exists U_{max} with $E[U_f(R_f(t))] \leq U_{max}$. Dividing (29) by $\epsilon \cdot T$, we have that

$$\begin{aligned} &\frac{1}{T} \sum_{t=0}^{T-1} E\left[\sum_f Q_f(t) + \sum_v Q_v(t) + \sum_l Q_l(t) + Q_p(t)\right] \\ &\qquad \leq \frac{E[\mathcal{L}(0)]}{\epsilon T} + \frac{B + V|F|U_{max}}{\epsilon}. \end{aligned} \tag{30}$$

Letting $T \to \infty$, we obtain the first result of (10).

For the second result, we rearrange (11) and similarly obtain that

$$\frac{1}{T} \sum_{t=0}^{T-1} \sum_f E[U_f(R_f(t))] \geq \sum_f U_f(\bar{R}^*_f) - \frac{B}{V} - \frac{E[\mathcal{L}(0)]}{VT}. \tag{31}$$

Letting $T \to \infty$, and from the convexity of $U_f(\cdot)$ and the Jensen's inequality, we can the second result. ■